Electronic supplementary information for

Highly efficient moisture-enabled electricity generation from graphene oxide frameworks

Fei Zhao, [a] Yuan Liang, [a] Huhu Cheng, [a] Lan Jiang, [b] and Liangti Qu*[a]

[a] Beijing Key Laboratory of Photoelectronic/Electrophotonic Conversion Materials, Key Laboratory of Cluster Science, Ministry of Education of China, Department of Chemistry, School of Science, Beijing Institute of Technology, Beijing 100081, P. R. China.

[b] Laser Micro-/Nano-Fabrication Laboratory, Beijing Institute of Technology, Beijing 100081, P. R. China.

*Corresponding author: lqu@bit.edu.cn

Preparation of 3D GO tablets. GO was synthesized using the modified Hummers method with a two-step purification process as reported previously.[S1] The 3D GO assembly was prepared by freeze-drying of the as-prepared GO dispersions (6 mg ml^{-1}, pH = 3–5) in polyethylene tubes with certain sizes for 3 days. The 3D GO tablet was prepared by tabletting of the 3D GO under a press of 30 kN for 3 min.

Structural polarization of 3D GO tablets. The 3D GO tablets was sandwiched by tow gold electrodes and set in an enclosed environment with a RH of 80 % under an applied voltage of 10 V for 180 s. After constant voltage polarization process, the as-prepared g-3D-GO tablets were in-situ shorted to eliminate the capacitance effect, where the circuit parameters were set as voltage = 0 V, time = 2000 s and step index = 10 points s^{-1}. Finally, the g-3D-GO tablets were dried in vacuum oven under 30 ºC for 2 h.

Measurement of the CPE harvesting process. The g-3D-GO tablet was sandwiched in two Al electrodes with vents and inserted to a test circuit in an enclosed container. Moisture carried by nitrogen and dry nitrogen was use to adjust RH. The circuit parameters of open circuit voltage test were current = 0 mA and step index = 5 points s^{-1}. The circuit parameters of short circuit current test were voltage = 0 mV and step index = 5 points s^{-1}.

Characterization. The morphology and element mapping of the samples was examined by scanning electron microscope (SEM, JSM-7001F). X-ray photolectron spectroscopy (XPS) data were recorded on an ESCALAB 250 photoelectron spectrometer (ThemoFisher Scientific) with Al Kα (1486.6 eV). X-ray diffraction

(XRD) patterns were obtained by using a Netherlands 1,710 diffractometer with a Cu Kα irradiation source (λ =1.54 Å). The voltage and current signals were recorded in real time using a Keithley 2400 multimeter, which was controlled by a LabView-based data acquisition system. The commercial solar cell is manufactured by SunPower Corporation.

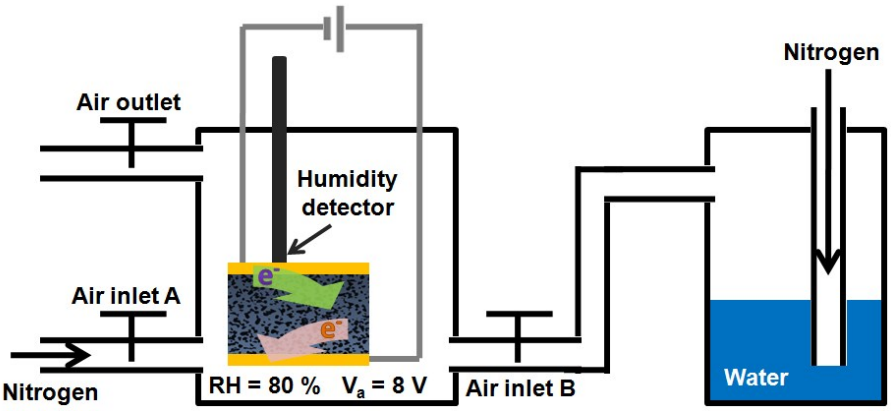

Fig. S1 Schematic illustration of the RH controlling system for structural polarization.

GO contains hydroxyl, epoxy (C-O) and carbonyl, carboxyl (C=O) groups. Among them, carboxyl and epoxy groups are reactive under reducing and oxidizing potential, respectively,[S2,S3] The top surface of GO assembly could be reduced while the bottom was oxidized. Meanwhile, GO thin films can release oxygen containing ions that migrated along with the electric field during the reduction reaction, constructing a gradient distribution.[S4,S5] However, in 3D-GO assemblies, electric field is not strong enough to force the migration of oxygen containing ions against the high ionic resistance, hence, the moisture was utilized to facilitate the ion migration by reducing the ionic resistance.

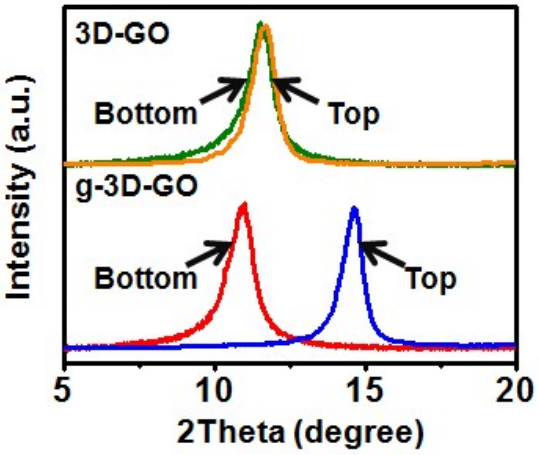

Fig. S2 XRD patterns of different sides of as-prepared 3D-GO and g-3D-GO (The surfaces of top and bottom in Figure 1 d to f are noted as *Top* and *Bottom*, respectively). X-ray diffraction (XRD) patterns of g-3D-GO reveal that the top and the bottom sides have the distinct peak shift nonanalogous to the initial 3D-GO, which suggests the structural polarization has indeed induced the change of interlayer structure. In contrast to 3D-GO with a calculated interlayer spacing of *ca.* 0.8 nm for both sides, the top and bottom sides of polarized 3D GO has an interlayer spacing of *ca.* 0.63 nm and *ca.* 0.9 nm, respectively, implying a partially reduced top GO layers and a slightly oxidized bottom layers of g-3D-GO in consistence with the corresponding element mapping (Figure 1e).

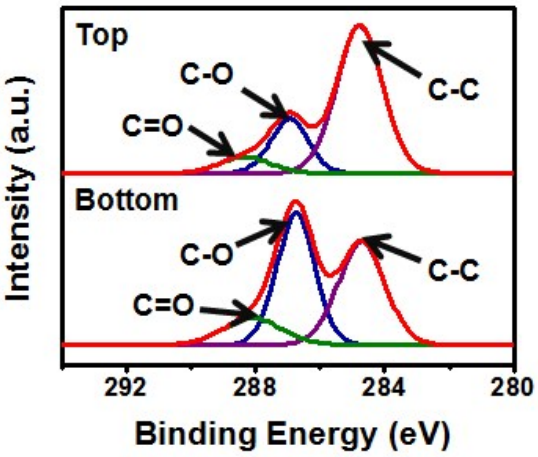

Fig. S3 XPS spectra of different surfaces of g-3D-GO (The surfaces of top and bottom in Figure 1 d to f are noted as *Top* and *Bottom*, respectively). The XPS survey spectra of both the top and bottom surfaces show predominant graphitic C 1s peak at *ca.* 284 eV and O 1s peak at ca. 532 eV. The O/C atomic ratio for the bottom side of g-3D-GO is *ca.* 0.56, slightly higher than that of GO starting material (*ca.* 0.44) but much higher than that of the top-surface (ca. 0.19), demonstrating the distribution variation of oxygen-containing groups from top to bottom as shown in Figure 1e. Moreover, the high resolution C 1s spectra confirmed the presence of C–O bands (286.6 eV) and C=O bands (288.5 eV) on both sides of g-3D-GO. The top side had the weakened C–O and C=O peaks, indicating that the oxygen-containing groups on the top layers of g-3D-GO were partially removed. At the meanwhile, the signals from bottom side presented the stronger C–O and C=O peaks, implying the increasing O/C atomic ratio of bottom side probably associated with the further oxidation. These results also explained the inconsistent interlayer spacing change of two sides of g-3D-GO observed by XRD as shown in Fig. S2.

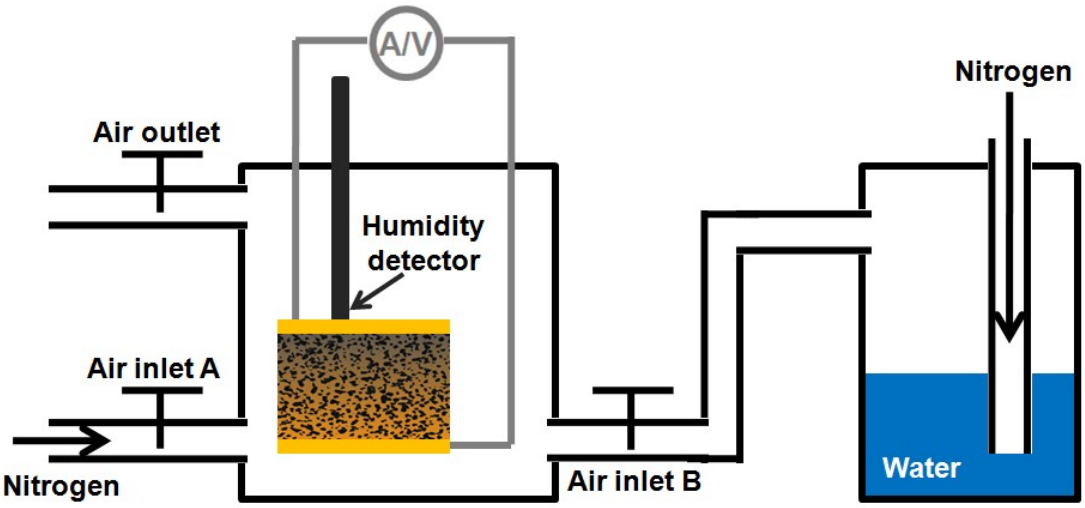

Fig. S4 Schematic illustration of the RH controlling system for structural polarization.

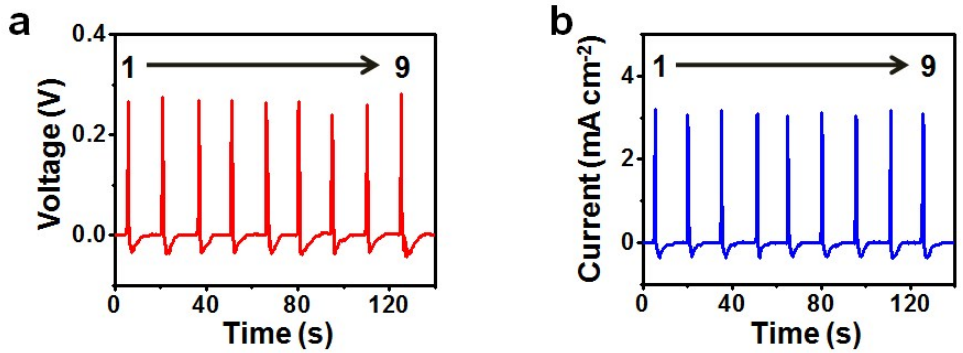

c

	1	2	3	4	5	6	7	8	9	Result
V_{max} (mV)	277	288	282	284	277	279	257	272	292	279±6.3
J_{max} (mA/cm²)	3.41	3.32	3.41	3.33	3.27	3.35	3.25	3.41	3.35	3.36±0.04

Confidence Interval = 95%

Fig. S5 Calculation of power density. (a) Voltage and (b) current output after 150 cycles of electric power generation. (c) Data list of voltage and current output and calculated value with confidence interval of 95%.

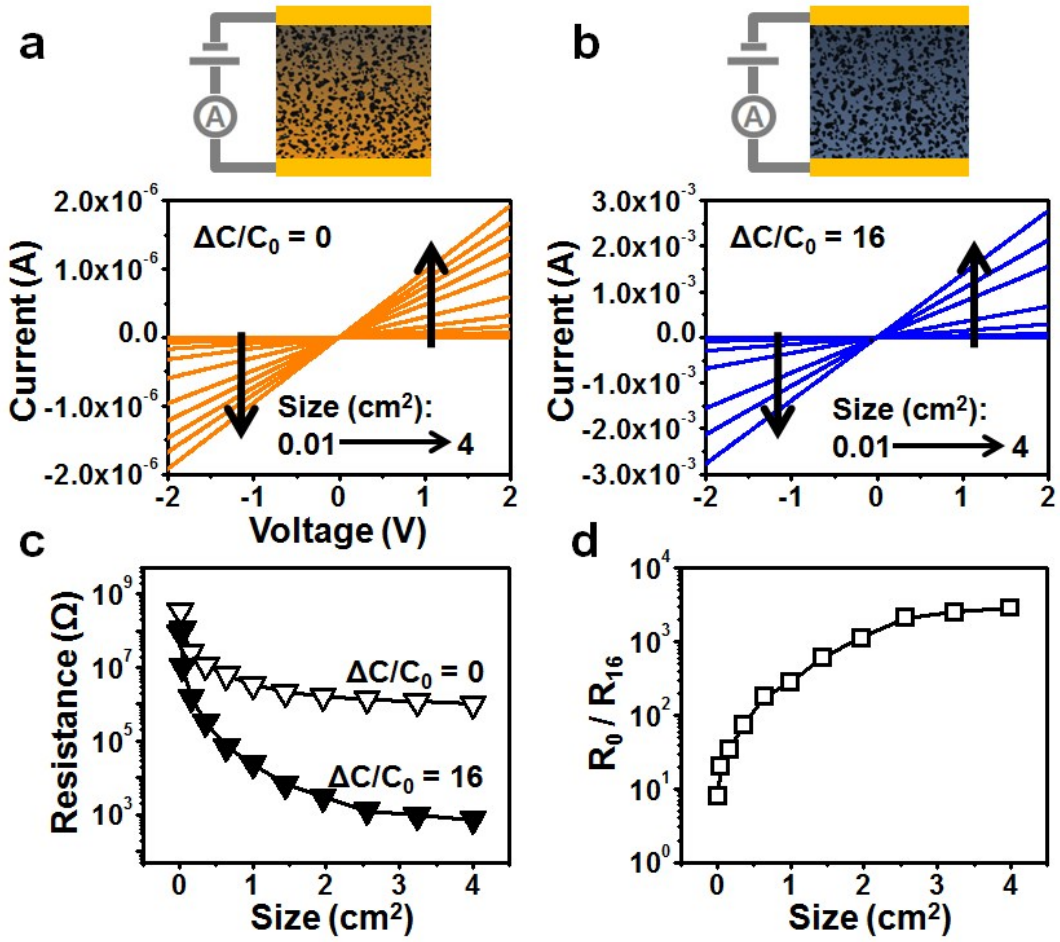

Fig. S6 Characterization of the water content dominated resistance. *I-V* characteristics of g-3D-GO with different size under (a) low $\Delta C/C_0$ (change of water content/initial water content) of 0 and (b) high $\Delta C/C_0$ of 16. (c) Dependence of resistance on CPEh size under low (0) and high (16) $\Delta C/C_0$. (d) Resistance ratio between dry and hydrated g-3D-GO, where R_0 and R_{16} represented resistance of g-3D-GO with $\Delta C/C_0$ of 0 and 16, respectively.

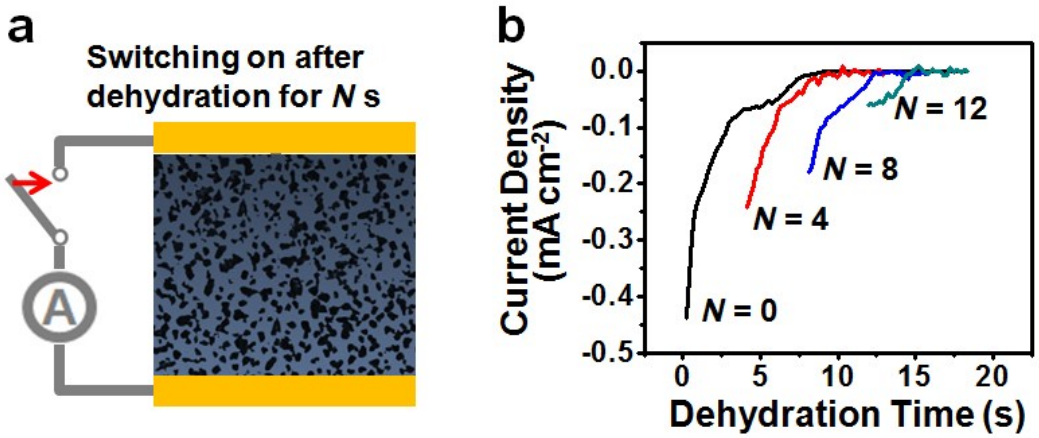

Fig. S7 Characterization of the internal relaxation of negative output. (a) Schematic illustration of experimental section for internal relaxation measurement. (b) Negative output after open-circuit dehydration for different time. It is demonstrated that the internal relaxation can quench the induced potential in g-3D-GO, and thus the negative output was negligible after c.a. 10 s.

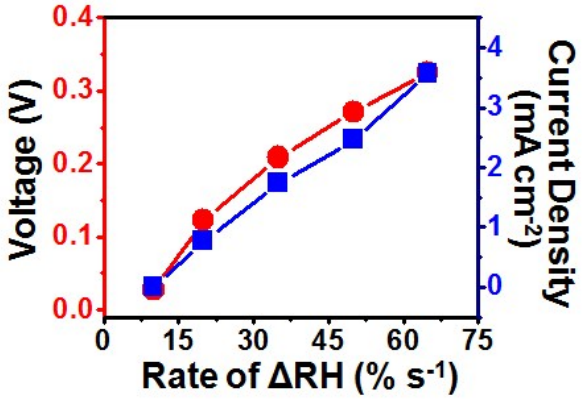

Fig. S8 The voltage and current output with different humidity changing rate. It is found that the output can be controlled by the humidity changing rate. Interestingly, the dependence between output and humidity changing rate is similar with the relationship of output and humidity variation, implying a dominance of humidity (i.e. water content) difference between g-3D-GO and environment in the power generation process.

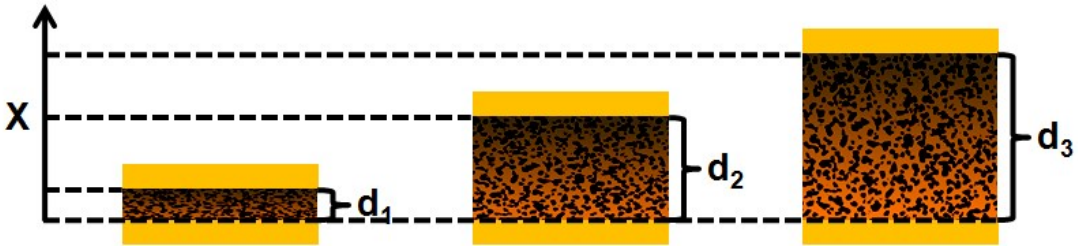

Fig. S9 Thermodynamic analysis of the thickness influence effect to voltage .

When the absorbed water filled g-3D-GO and disassociated the $H^{\delta+}$, the gradient distribution of $H^{\delta+}$ will enabled a diffusion process which could be described as:

$$J_{dif} = -qD\frac{dc}{dx} \quad \text{(S1)}$$

where the J_{dif}, q, D, c and x were diffusion current density, electric quantity of elementary charge, diffusion coefficient, concentration of $H^{\delta+}$ and distance between two surfaces of g-3D-GO, respectively.[S1] Meanwhile, the drift induced electric field between two sides of g-3D-GO will arise once the $H^{\delta+}$ reached the O-poor part, which could be defined by:

$$J_{dri} = \sigma E_i \quad \text{(S2)}$$

where the J_{dri}, σ and E_i were drift current density, conductivity and induced electric field intensity, respectively.[S1] When the thermodynamic equilibrium was established, we get:

$$J_{dif} + J_{dri} = 0 \quad \text{(S3)}$$

Therefore, the final equation is:

$$E_i = \frac{qD}{\sigma} \cdot \frac{dc}{dx} \quad \text{(S4)}$$

Considering an x-axis perpendicular to the surface of g-3D-GO, the induced voltage U_i could be described as:

$$U_i = \int \frac{qD}{\sigma} \cdot \frac{dc}{dx} \quad \text{(S5)}$$

where we suppose the absorbed water is able to provide enough transport channels to guarantee same diffusion coefficient and ionic conductivity in each part of g-3D-GO.

It means that the diffusion coefficient and ionic conductivity are not functions of x, and hence the reduced final equation is:

$$U_i = \frac{qD}{\sigma} \cdot \int \frac{dc}{dx} \quad \text{(S6)}$$

indicating that the intensity of induced voltage was directly defined by gradient of $H^{\delta+}$ which was created by O-gradient of g-3D-GO. Meanwhile, since the *c* is dominated by the oxygen-containing group density in g-3D-GO, the value range (concentration difference of $H^{\delta+}$, i.e. Δc) of *c* and value of *dc/dx* were defined once the structural polarization is finished. As a result, the U_i is proportional to the value range of *x*, i.e. desistance between the electrodes.

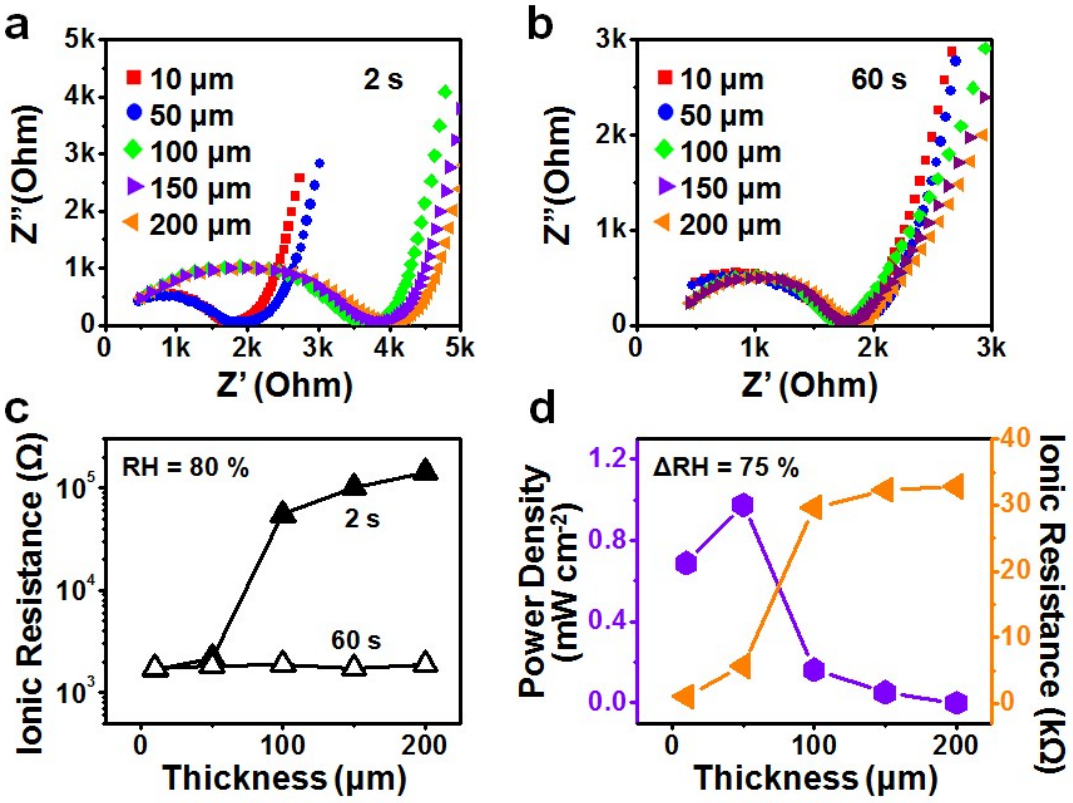

Fig. S10 Characterization of the thickness effect on g-3D-GO based CPEhs. (a) Dependence of ionic resistance on g-3D-GO thickness with short (2 s) and long (60 s) exposure time to high RH environment (80 %). (b) Relationship between electric output efficiency and ionic resistance with different thickness of g-3D-GO in response to the RH variation (ΔRH = 75 %). The evolution of the impedance spectra of g-3D-

GO with different thickness exposing to moisture under relative humidity of 80 % for (c) 2s and (d) 60s, 1 MHz to 10 mHz at 10 mV sinusoidal signal, zoomed in at the high frequency region.

Considering that the ionic diffusion in g-3D-GO was affected by the water assistant ionic conduction, the impedance spectroscopy measurements were conducted on the g-3D-GO with certain thickness to study the hydration dependent variation of ionic conductivity. For the ionic conductivity measurement, the impedance spectra obtained turned out to be a depressed semicircle with a slanted line at lower frequencies as shown in Fig. S7 a and b. In solid electrolyte system, the corresponding equivalent circuit for this type of spectra is typically represented by electrode resistance in series with a parallel combination of electrolyte resistance and capacitance. Therefore, our impedance data at high frequencies were fitted by Z-view according to this equivalent circuit, where the depressed semicircles were simulated by the electrolyte resistance in parallel with a Constant Phase Element (CPE) that is generally a result of electrode roughness. As shown in Fig. S7 c, when the g-3D-GOs with different thickness were exposed to high RH environment (80 %) for 60 s, their ionic resistances were stabilized around 2×10^3 Ω. In contrast, although the g-3D-GOs with thickness of 10 and 50 μm maintained the low ionic resistance when the exposed time was shortened to 2 s (time for power generation), the relatively thicker samples presented higher ionic resistance of about 1×10^5 Ω, indicating a poor ionic conductivity. Additionally, in view of the uniform distribution of oxygen-containing groups, it is reasonable to approximate the *dc/dx* to *Δc* in equation S1 and hence the reduced final equation is:

$$J_{dif} = -qD\Delta c \quad \text{(S7)}$$

which means that the current is proportional to the ionic conductivity of the g-3D-GO. As a result, the maximum output power density was provided by the g-3D-GOs with a thickness of 50 μm (Fig. S7 d)

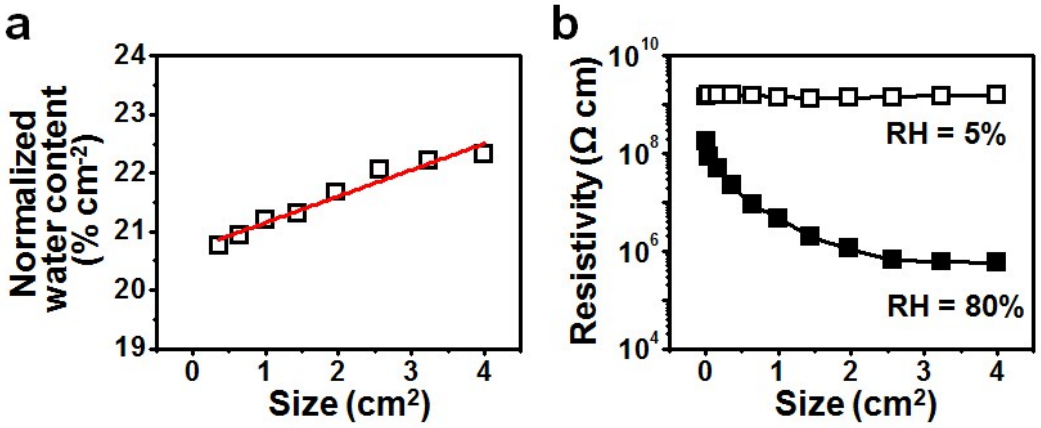

Fig. S11 The enhancement and reduction effects of output that induced by size increasing. (a) The water content per unit area of samples with different sizes. (b) resistivity variation of samples with different sizes under specific humidity.

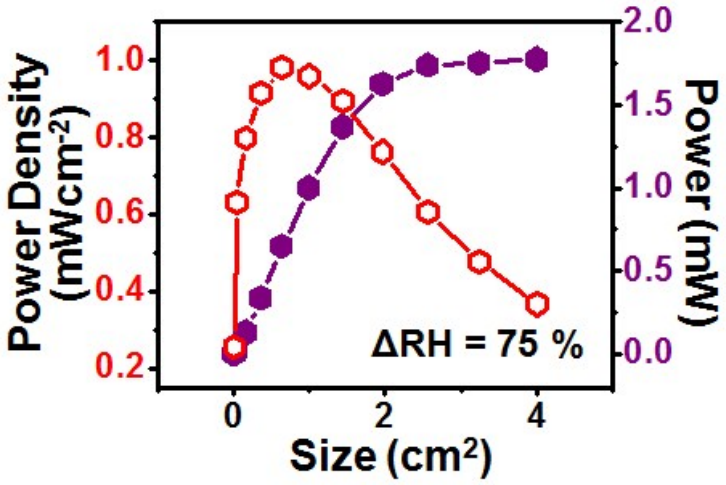

Fig. S12 Characterization of the size effect on g-3D-GO based CPEhs. Relationship between electric output power density and output power with different sample size in response to the RH variation (ΔRH = 75 %). This nonlinear size/output dependency leads to a contradictory between output power density and actually generated power. The experimental data of power and power density reached a balance around 1.7 cm^2, which hence was proposed as an optimal size of a single CPEh cell.

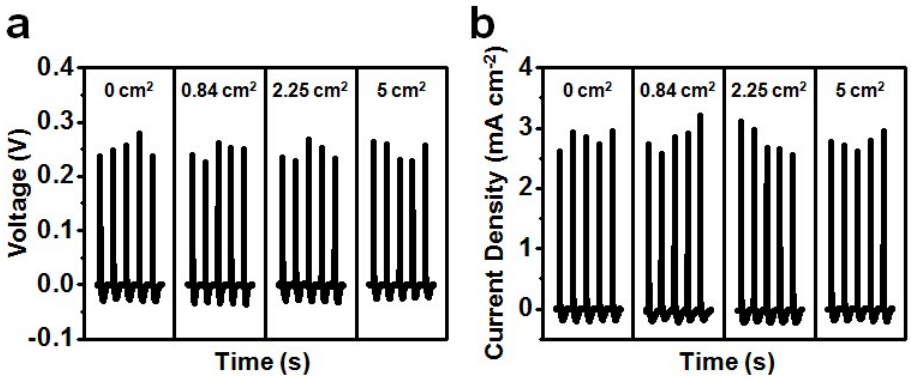

Fig. S13 Influences on device signals by the capacitive reactance effect of insulating cement. (a) Voltage and (b) current output of packaged devices with different cement size of 0 to 5 cm2. In current work, the size of cement didn't affect the device performance.

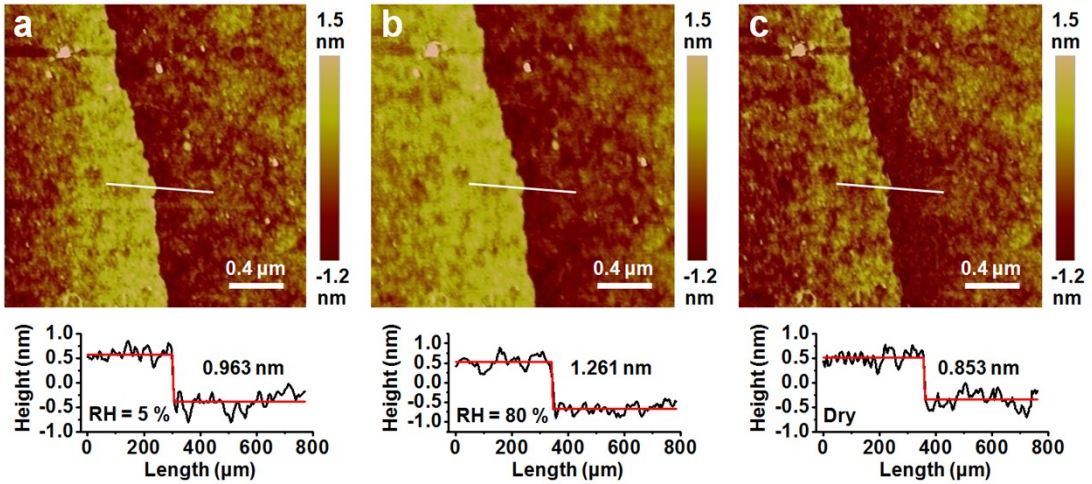

Fig. S14 Water adsorption of GO single sheet. AFM image with corresponding height information of GO single sheet on SiO_2 substrate exposing to (a) ambient (RH = 5 %), (b) moisture (RH=80 %) and (c) dry nitrogen blow. The difference of average height is ca. 0.4 nm, which equals to the thickness of a layer of water molecule.

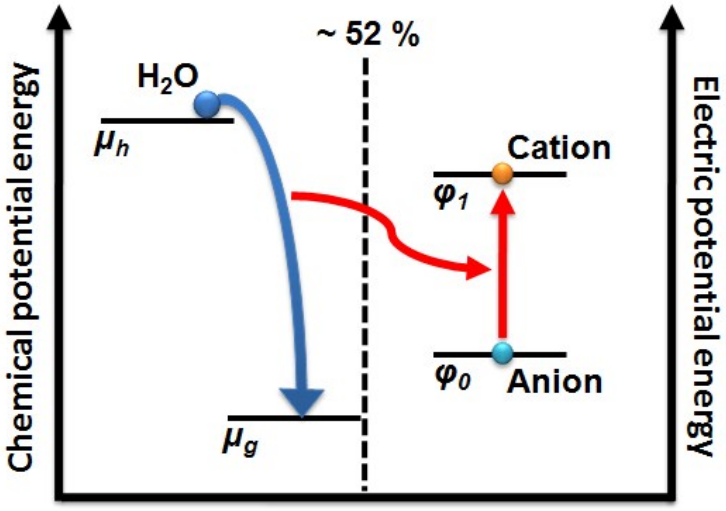

Fig. S15 Energy conversion diagram.

I. Calculation of input energy. The chemical potential of water in a high RH environment μ_h and in the g-3D-GO μ_g in a descending order are: $\mu_h > \mu_g$. When an as-prepared g-3D-GO contact with moisture in high RH environment, the Gibbs free energy change of absorbed water were $\Delta G_a = \mu_g - \mu_h < 0$, indicating a spontaneous CPE absorption. Considering that there is no additional energy in CPE harvesting, the ΔG_a is the sole energy source for the energy conversion process, and also defines the maximum capability of the generated electric output.

$$\Delta G_{ag} = \mu_h - \mu_g \approx RTln\frac{C_0}{C_0 - \Delta C} \quad \text{(S8)}$$

where R, T and C_0 are ideal gas constant, Kelvin temperature and the concentration of water in high RH environment, respectively. Since the environmental RH is tested as 80 %, C_0 should be 10.2 g m^{-3} at 282 K (experimental condition). Meanwhile, the water concentration in g-3D-GO could be calculated from the mass of adsorbed water / the volume of g-3D-GO tablet, hence the obtained ΔC is ca. 2.5 g m^{-3}. As a result, we get $\Delta G_a \approx$ -2.12 J mol^{-1} at 283 K. Meanwhile, in view of the fast water adsorption

process within 1 s and the thickness limitation of g-3d-GO, the calculated CPE absorption efficiency is 1.76 mW cm^{-2}

II. Calculation of internal energy conversion efficiency. The electric potential of free cations that separated from confined anion φ_1 and cations that trapped by confined anions φ_0 in a descending order are: $\varphi_1 > \varphi_0$. When the CPE force the dissociation of cationic-anionic pairs, the Gibbs free energy change of cationic-anionic pairs were $\Delta G_{ca} = \varphi_0 - \varphi_1 < 0$, indicating a spontaneous CPE conversion. Considering that there is no additional energy in CPE harvesting, the ΔG_{ca} is the sole energy source for the electric power generation The power output (W_{CPE}) of CPE conversion can be calculated as:

$$W_{meg} = \int J_{sc}(t) \cdot V_{oc}(t)\, d(t) \quad \text{(S9)}$$

where J_{sc}, V_{oc} and t are the short-circuit current density, open-circuit voltage and the time of cycle, respectively. The calculation results showed *ca.* 0.91 mW cm^{-2} and the CPE harvesting efficiency is *ca.* 51.71%.

References

S1. F. Zhao, H. Cheng, Z. Zhang, L. Jiang, L. Qu, *Adv. Mater.* 2015, **27,** 4351–4357.

S2. F. Zhao, J. Q. Liu, X. Huang, X. Zou, G. Lu, P. J. Sun, S. X. Wu, W. Ai, M. D. Yi, X. Y. Qi, L. H. Xie, J. L. Wang, H. Zhang, W. Huang, *ACS Nano* 2012, **6**, 3027–3031.

S3. S. Seo, Y. Yoon, J. Lee, Y. Park, H. Lee, *ACS Nano* 2013, **7**, 3607–3615.

S4. H. Y. Jeong, J. Y. Kim, J. W. Kim, J. O. Hwang, J. E. Kim, J. Y. Lee, S. Y. Choi, *Nano Lett.* 2010, **10**, 4381–4386.

S5. F. Zhao, H. Cheng, Z. Zhang, L. Jiang, L. Qu, *Adv. Mater.* 2015, **27**, 4351–4357.